Supplementary Information

Slowdown of typhoon translation speed and its links to the storm poleward migration

Xiangbo Feng[1,2]*

[1] National Centre for Atmospheric Science and Department of Meteorology, University of Reading, Reading, UK.

[2] Department of Physics, Imperial College London, London, UK.

*Corresponding author: Xiangbo Feng (xiangbo.feng@reading.ac.uk)

Supplementary Information Table S1: Trend values of basin-wide translation speed of typhoons in observations in 1980–2023.

Trends of TC translation speed (TCS) in the western North Pacific, based on Japan Meteorological Agency (JMA) Best Track data in 1980–2023. The TCS is partitioned to three components related to regional track density ($\delta_{p'}$), regional TCS ($\delta_{TCS'}$), and co-variations of regional track density and regional TCS ($\delta_{p'TCS'}$), respectively. The sum of the trends in the three terms is also provided to examine the trend budget closure. TCS is also partitioned to latitudinal and longitudinal components, representing the meridional and zonal propagation speed. The El Niño Southern Oscillation (ENSO) and Pacific Decadal Oscillation (PDO) effects have been removed with a multivariate regression before estimating the trend; ± represents the 95% confidence interval of trend value, with bold indicating significant trend at the 95% confidence.

1980–2023	TCS (km/h/decade)	Latitudinal TCS (km/h/decade)	Longitudinal TCS (km/h/decade)
Total TCS	**-0.63±0.37**	-0.09±0.25	**-0.67±0.30**
TCS $\delta_{p'}$	**0.23±0.17**	**0.27±0.11**	0.05±0.13
TCS $\delta_{TCS'}$	**-0.88±0.45**	**-0.37±0.28**	**-0.74±0.38**
TCS $\delta_{p'TCS'}$	0.02±0.16	0.00±0.11	0.02±0.14
Sum ($\delta_{p'}$, $\delta_{TCS'}$, $\delta_{p'TCS'}$)	**-0.63**	-0.09	**-0.67**

Supplementary Information Table S2: Interannual variability of basin-wide translation speed of typhoons in observations in 1980–2023.

Interannual variability amplitude (standard deviation) of TC translation speed (TCS) in the western North Pacific, based on Japan Meteorological Agency (JMA) Best Track data in 1980–2023. The TCS is partitioned to three components related to regional track density ($\delta_{p'}$), regional TCS ($\delta_{TCS'}$), and co-variations of regional track density and regional TCS ($\delta_{p'TCS'}$), respectively. Interannual variability of the sum of the three terms is also provided to examine the variability budget closure. TCS is also partitioned to latitudinal and longitudinal components, representing the meridional and zonal propagation speed. The El Niño Southern Oscillation (ENSO) and Pacific Decadal Oscillation (PDO) effects have been removed with a multivariate regression before estimating the variability.

1980–2023	TCS (km/h)	Latitudinal TCS (km/h)	Longitudinal TCS (km/h)
Total TCS	1.75	1.06	1.52
TCS $\delta_{p'}$	0.76	0.58	0.56
TCS $\delta_{TCS'}$	2.19	1.26	1.86
TCS $\delta_{p'TCS'}$	0.66	0.46	0.60
Sum ($\delta_{p'}$, $\delta_{TCS'}$, $\delta_{p'TCS'}$)	1.75	1.06	1.52

Supplementary Information Table S3: Trend values of basin-wide latitudinal position and translation speed of typhoons in multiple sources of Best Track data in 1980–2021.

Trends of basin-wide TC latitudinal position and translation speed (TCS) in the western North Pacific, based on four sources of Best Track data in the common period of 1980–2021. Four data sources are the Japan Meteorological Agency (JMA), China Meteorological Administration (CMA), Joint Typhoon Warning Centre (JTWC), and Hong Kong Observatory (HKO). The TCS is partitioned to three components related to regional track shift ($\delta_{p'}$), regional TCS trend ($\delta_{TCS'}$), and co-variations of regional track density and regional TCS ($\delta_{p'TCS'}$), respectively. The El Niño Southern Oscillation (ENSO) and Pacific Decadal Oscillation (PDO) effects have been removed with a multivariate regression before estimating the trend; ± represents the 95% confidence interval of trend value, with bold indicating significant trend at the 95% confidence.

1980–2021	JMA	CMA	JTWC	HKO
Latitudinal position	**82±36**	**85±31**	**40±33**	**38±31**
Total TCS	**-0.60±0.42**	-0.06±0.38	0.01±0.36	-0.02±0.38
TCS $\delta_{p'}$	**0.27±0.17**	**0.42±0.21**	0.16±0.22	0.10±0.16
TCS $\delta_{TCS'}$	**-0.89±0.51**	-0.34±0.48	-0.08±0.39	-0.05±0.40
TCS $\delta_{p'TCS'}$	0.02±0.17	-0.13±0.13	-0.07±0.13	-0.08±0.10

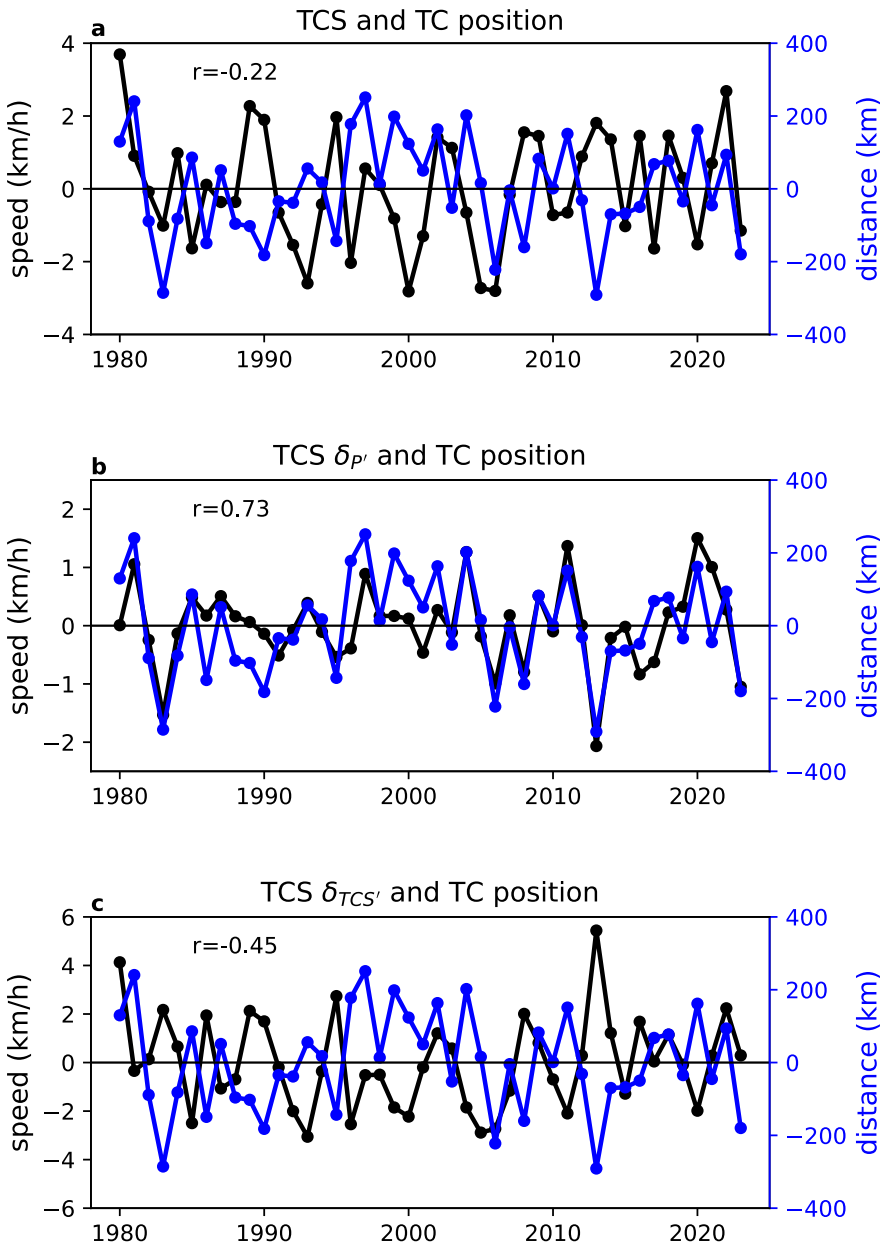

Supplementary Information Fig.S1: Detrended interannual variability of basin-wide translation speed and latitudinal position of typhoons in observations.

a, Detrended annual values of tropical cyclone translation speed (TCS, black) and tropical cyclone latitude (blue) in the western North Pacific over 1980–2023, from the 6-hourly track points in the Best Track. **b** and **c** as **a**, but with black line for basin-wide TCS related to track shift ($\delta_{p'}$) and basin-wide TCS related to regional TCS change ($\delta_{TCS'}$), respectively. Dashed lines represent the linear trend, with shading showing 95% confidence interval for the linear fit. Correlation coefficient between detrended TCS and TC position timeseries is provided in top left.

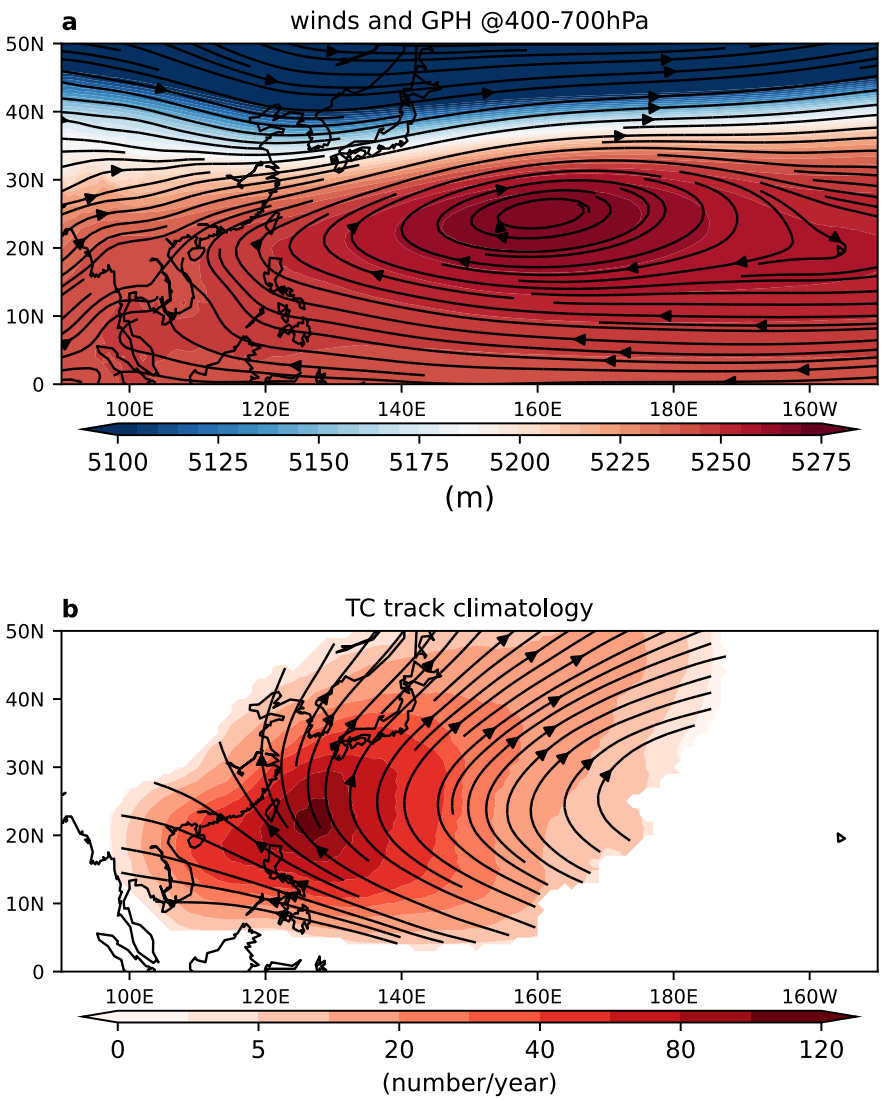

Supplementary Information Fig.S2: Climatology of large-scale steering flow and typhoon movement in observations.

a, Climatology of annual geopotential height (GPH; shading) and annual steering wind streamlines (vectors) averaged over 700, 600, 500, and 400hPa, over 1980–2023, in ERA5. The annual circulation and environment are calculated by integrating the monthly data weighted with the monthly proportion of WNP TC frequency throughout the 12 months. **b**, Climatology of TC track density (shading) and TC movement streamlines (vectors) in the WNP over 1980–2023, from the 6-hourly track points in the Best Track. Regional track density is calculated at each grid point as the annual number of 6-hourly translation speed samples over an area defined by a 10° × 10° box centred at the grid point, per year. Regional TC movements are calculated at each grid point as the longitudinal and latitudinal TC translation velocities averaged over an area defined by a 10° × 10° box centred at the grid point.

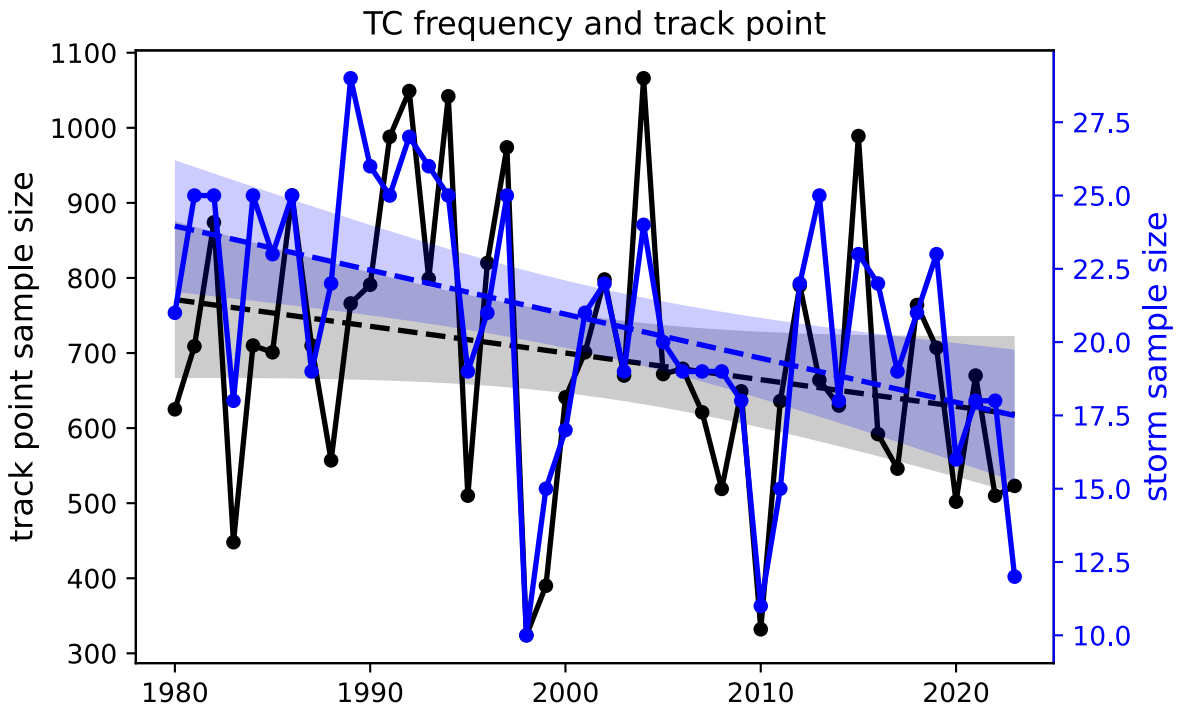

Supplementary Information Fig.S3: Sample size of typhoon frequency and 6-hourly track points in observations.

Annual number of tropical cyclone frequency (blue) and 6-hourly track points (black) used for translation speed in the western North Pacific over 1980–2023, from the Best Track. Dashed lines represent the linear trend, with shading showing 95% confidence interval for the linear trend.

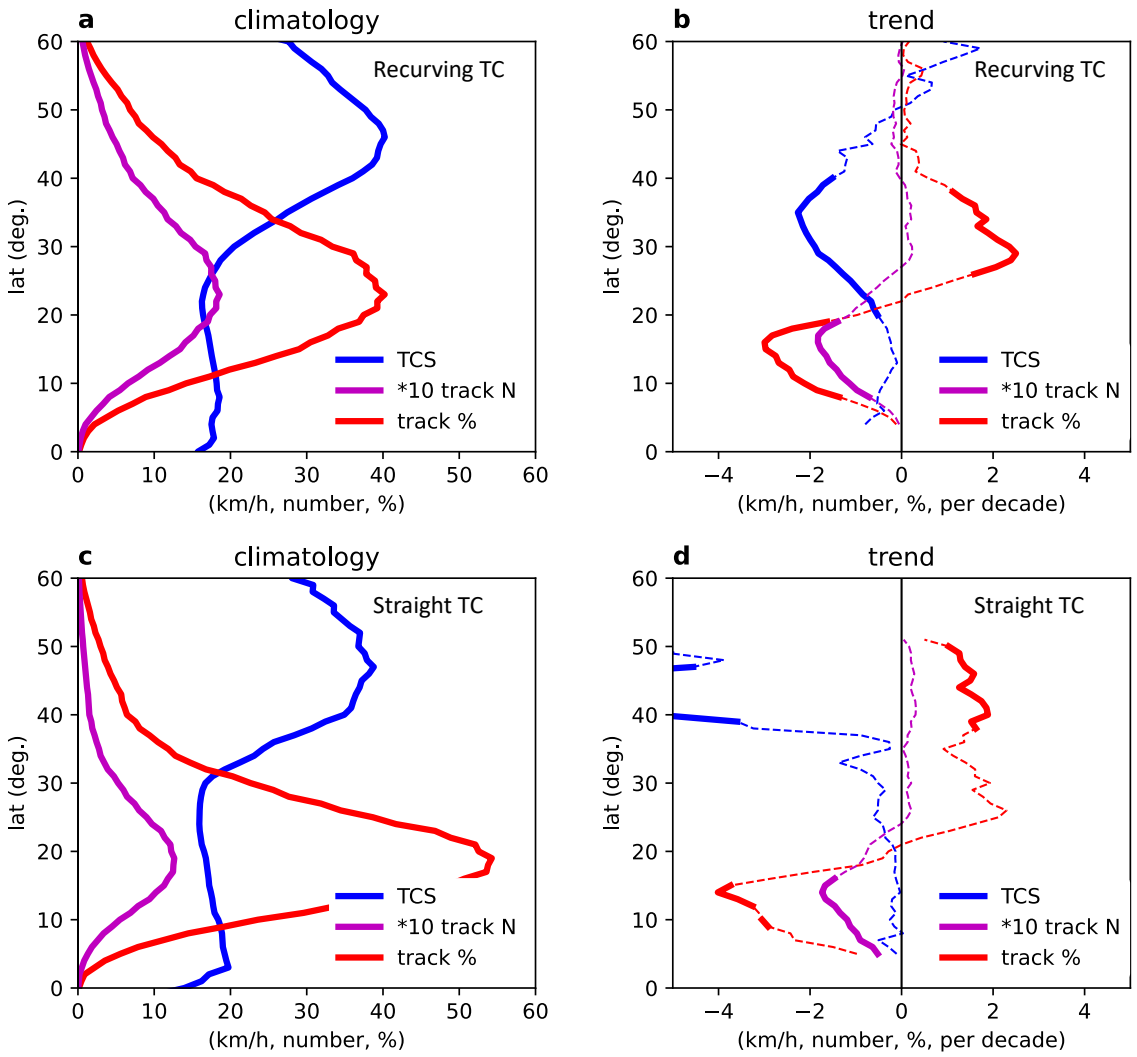

Supplementary Information Fig.S4: Climatology and long-term changes in translation speed and track density, for recurving and straight-moving typhoons, at the latitude bands in observations.

a, Climatology of tropical cyclone translation speed (TCS, blue line), track density (magenta line), and the proportion of track density (red line), at the 10° latitude-moving bands from 0 to 60°N, for recurving storms, in the WNP over 1980–2023, from the 6-hourly track points in the Best Track. **b,** Linear trends of TCS (blue line), track density (magenta line), and the proportion of track density (red line), at the 10° latitude-moving bands from 0 to 60°N, for recurving storms, in the WNP over 1980–2023, from the 6-hourly track points in the Best Track. **c** and **d**, as **a** and **b**, but for straight-moving storms. In **b** and **d**, thick solid lines show significant trends at 95% confidence, thin dashed lines for insignificant trends at 95% confidence.

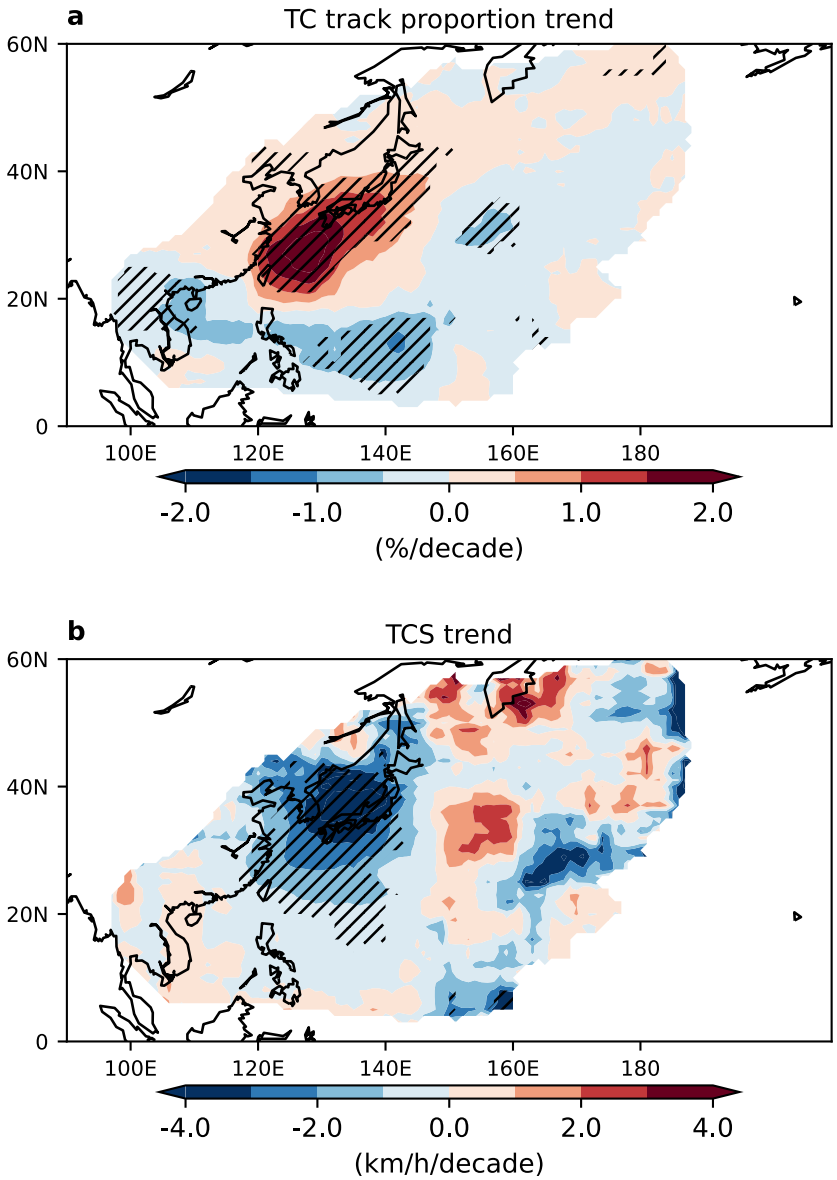

Supplementary Information Fig.S5: Long-term changes in relative track density and translation speed of typhoons at regional scales in observations.

a, Linear trends of the proportion of TC track density, in the WNP over 1980–2023, from the 6-hourly track points in the Best Track. **b,** Linear trends of regional TC translation speed (TCS), in the WNP over 1980–2023, from the 6-hourly track points in the Best Track. Hatched areas show significant trends at 95% confidence. Regional relative track density is calculated at each grid point as the percentage of the annual number of track points in an area (defined by a 10° × 10° box centred at the grid point) over the total number of track points in the whole basin, for each year. Regional TCS is calculated at each grid point as the annual TCS averaged over an area (defined by a 10° × 10° box centred at the grid point), for each year.

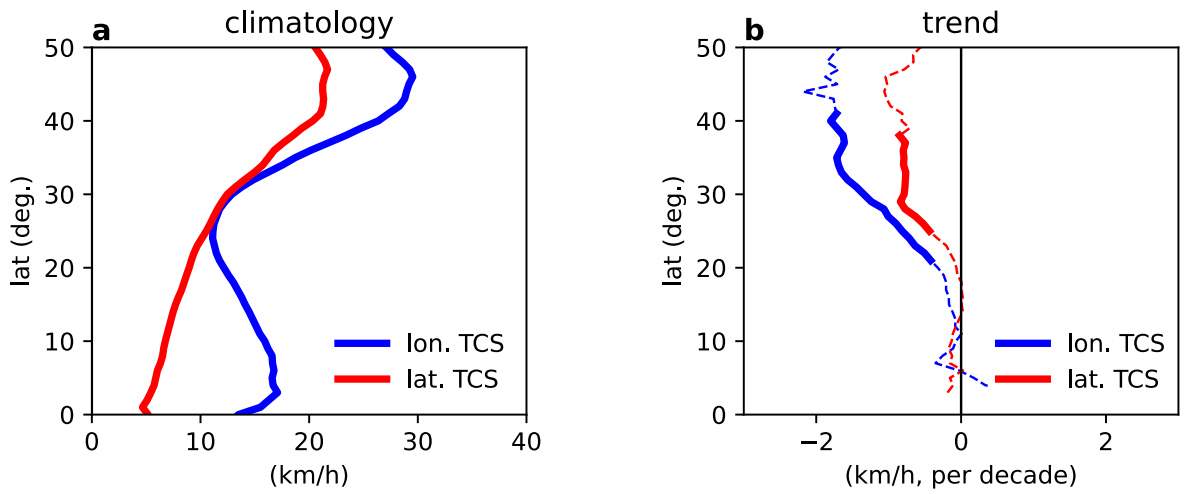

Supplementary Information Fig.S6: Climatology and long-term changes in longitudinal and latitudinal translation speed of typhoons at the latitude bands in observations. **a**, Climatology of tropical cyclone longitudinal translation speed (longitudinal TCS, blue line) and latitudinal translation speed (latitudinal TCS, red line), at the 10° latitude-moving bands from 0 to 60°N, in the western North Pacific over 1980–2023, from the 6-hourly track points in the Best Track. **b**, Linear trends of longitudinal TCS (blue dashed line) and latitudinal TCS (red dashed line), at the 10° latitude-moving bands from 0 to 60°N, in the western North Pacific over 1980–2023 from the 6-hourly track points in the Best Track. In **b**, thick solid lines show significant trends at 95% confidence, thin dashed lines for insignificant trends at 95% confidence.

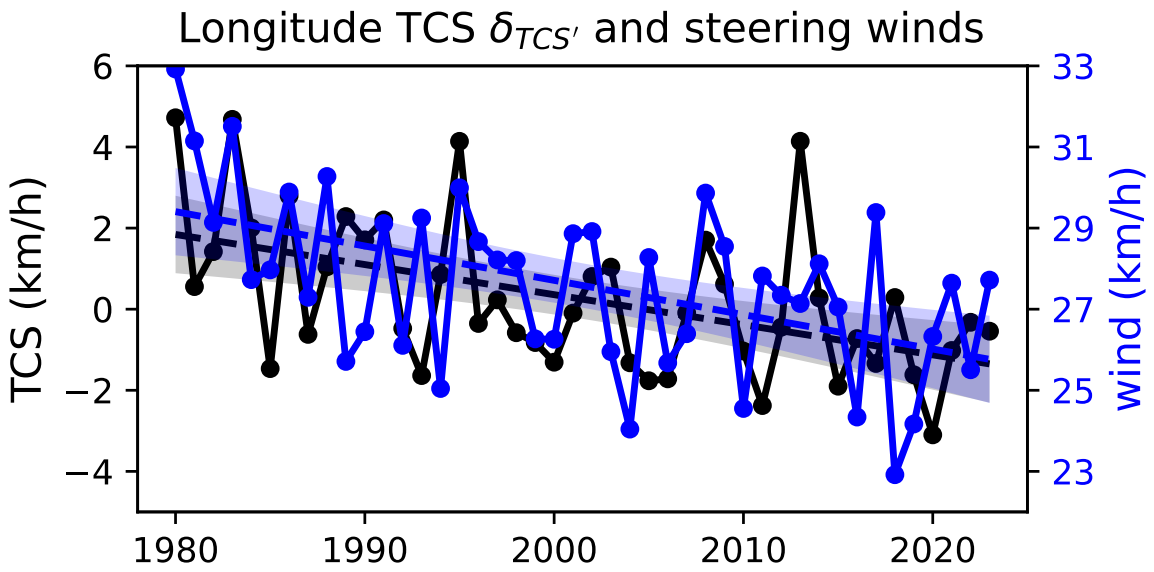

Supplementary Information Fig.S7: Changes in basin-wide longitudinal translation speed of typhoons and the large-scale steering flow.

Annual deviations of basin-wide TC longitudinal translation speed (longitudinal TCS) related to regional TCS change ($\delta_{TCS'}$, black line) in the Best Track, and annual values of the large-scale steering flow (blue line) averaged over 700, 600, 500, and 400hPa in the northwest sector (20–40°N, 120–160°E) of the basin in ERA5, over 1980–2023. Dashed lines represent the linear trend, with shading showing 95% confidence interval for the linear trend. The annual large-scale steering flow is calculated by integrating the monthly steering flow weighted with the monthly proportion of WNP TC frequency throughout the 12 months.

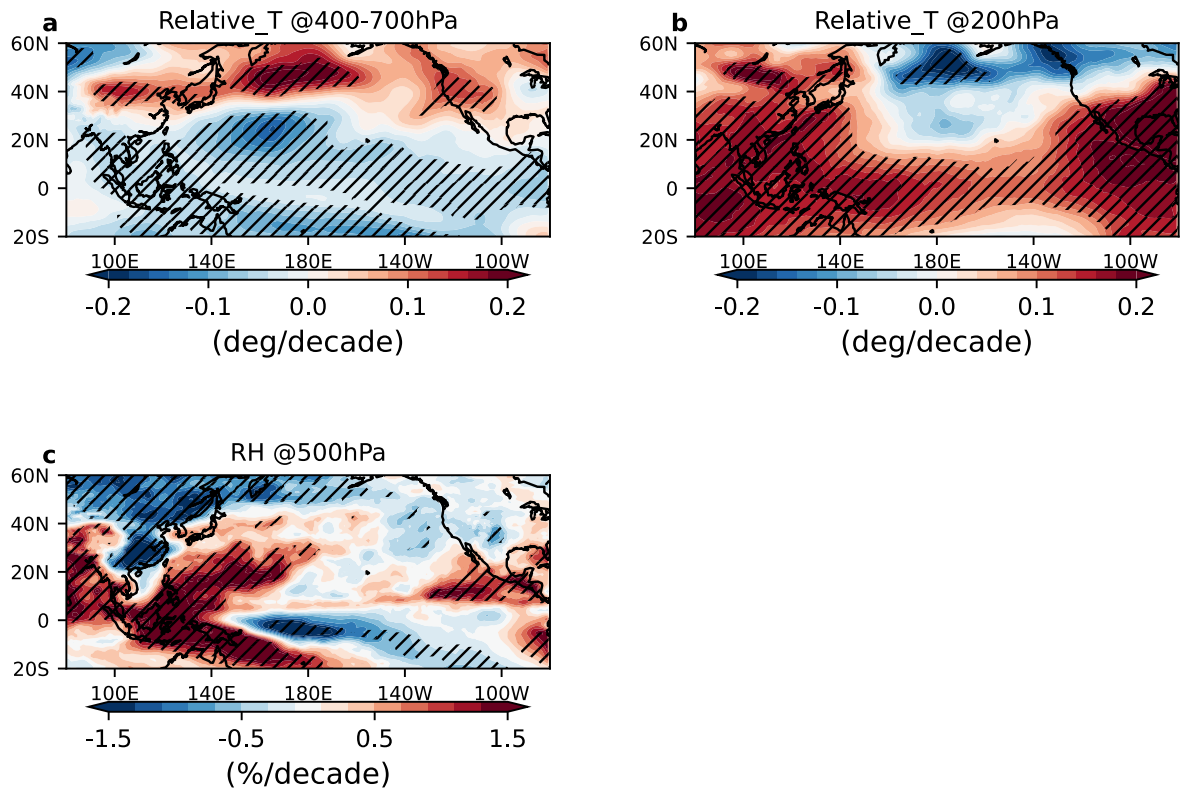

Supplementary Information Fig.S8: Long-term changes in large-scale environment. **a**, Linear trends of annual air temperature relative to the global mean (Relative_T; shading) averaged over 700, 600, 500, and 400hPa, over 1980–2023, in ERA5. **b** as **a**, but for air temperature relative to the global mean (Relative_T; shading) at 200hPa. **c** as **a**, but for relative humidity (RH; shading) at 500hPa. Hatched areas show significant trends at 90% confidence. The annual environment is calculated by integrating the monthly data weighted with the monthly proportion of WNP TC frequency throughout the 12 months.

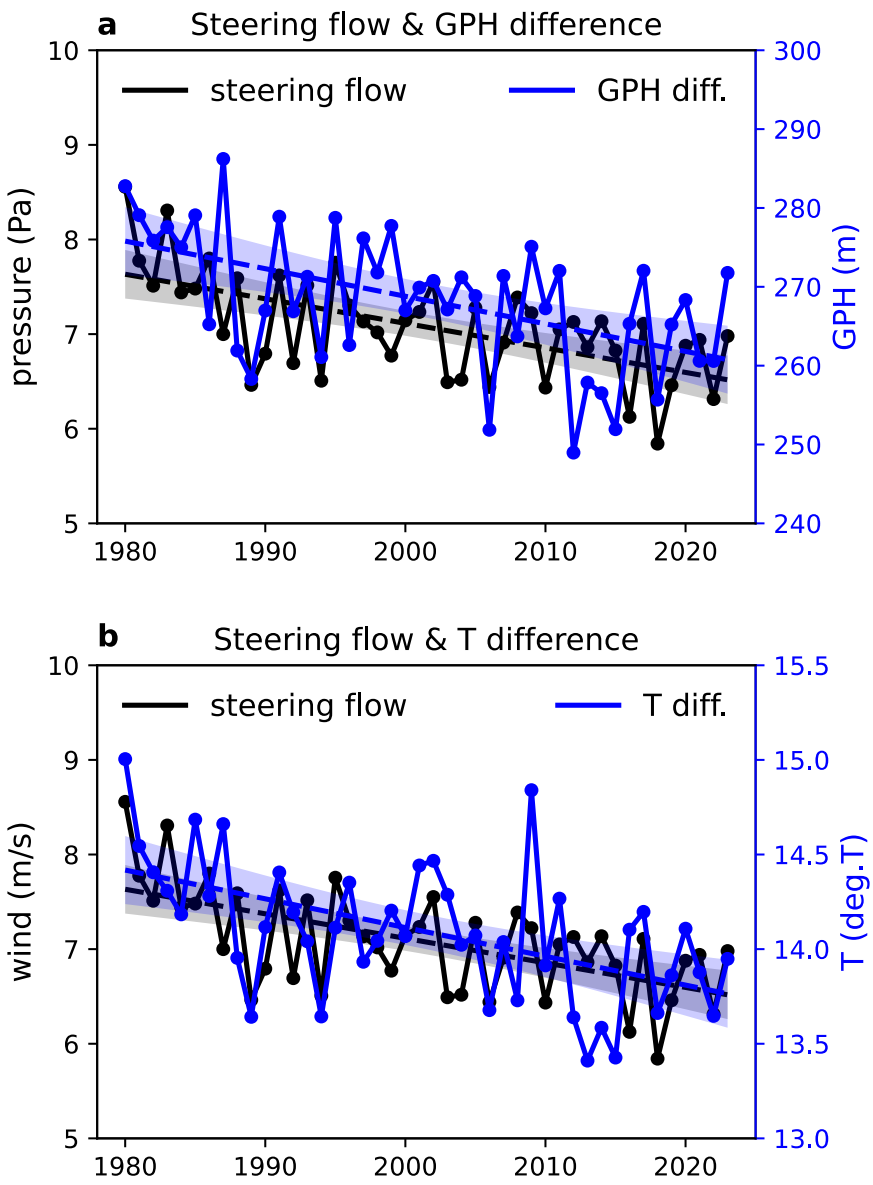

Supplementary Information Fig.S9: Changes in large-scale steering flow.

a, Values of the large-scale steering flow (black line) in the northwest sector (20–40°N, 120–160°E) of the basin, and values of geopotential height (GPH) difference (blue line) between the high (60–40°N, 120–160°E) and low latitude (0–20°N, 120–160°E) regions, over 1980–2023, in ERA5. **b** as **a**, but with blue line for air temperature difference. The steering flow, GPH, and air temperature are averaged over 700, 600, 500, and 400hPa. The annual circulation and environment are calculated by integrating the monthly data weighted with the monthly proportion of WNP TC frequency throughout the 12 months. Dashed lines represent the linear trend, with shading showing 95% confidence interval for the linear trend.

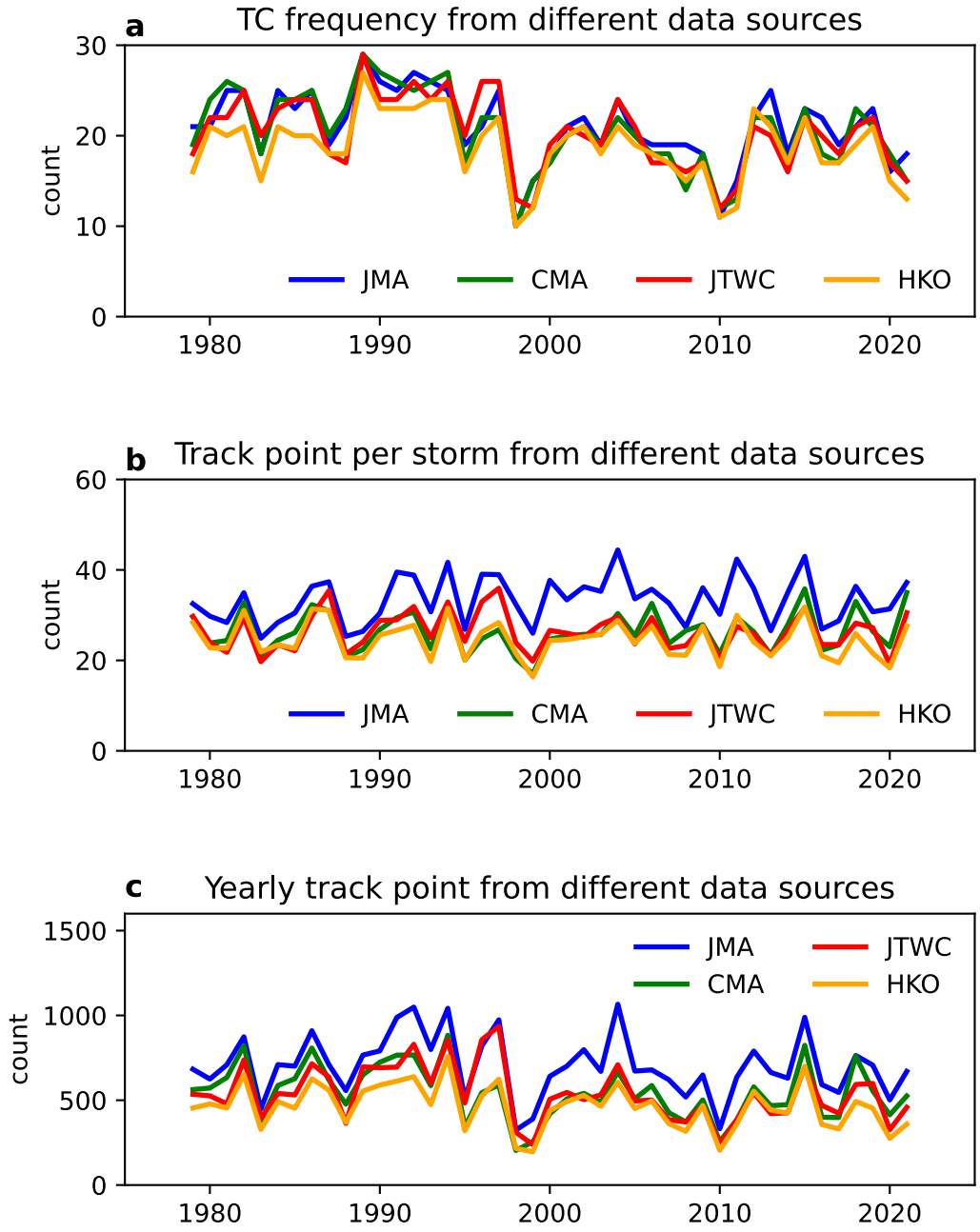

Supplementary Information Fig.S10: TC frequency and track point counts from different Best Track data sources in the common period of 1980–2021.

a, Annual TC frequency in the western North Pacific from different Best Track data sources, including the JMA, CMA, JTWC and HKO, in the common period of 1980–2021. **b** and **c** as **a**, but for the average number of track points per TC, and the annual total number of track points, respectively.

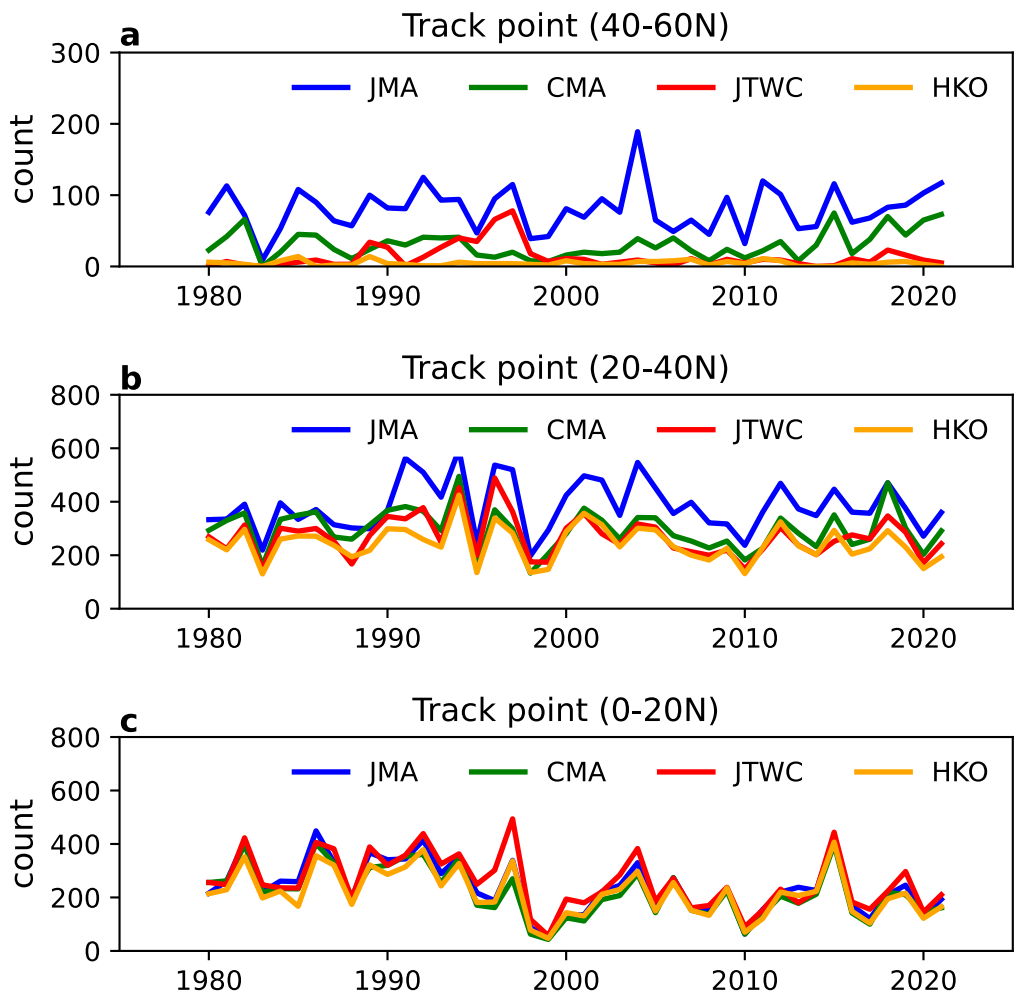

Supplementary Information Fig.S11: TC track point counts in various latitudinal bands from different Best Track data sources in the common period of 1980–2021.

a, The annual total number of track points falling within the latitudinal band of 40–60°N in the WNP from different Best Track data sources, including the JMA, CMA, JTWC and HKO, in the common period of 1980–2021. **b** and **c** as **a**, but for the annual total number of track points falling within the bands of 20–40°N and 0–20°N, respectively.

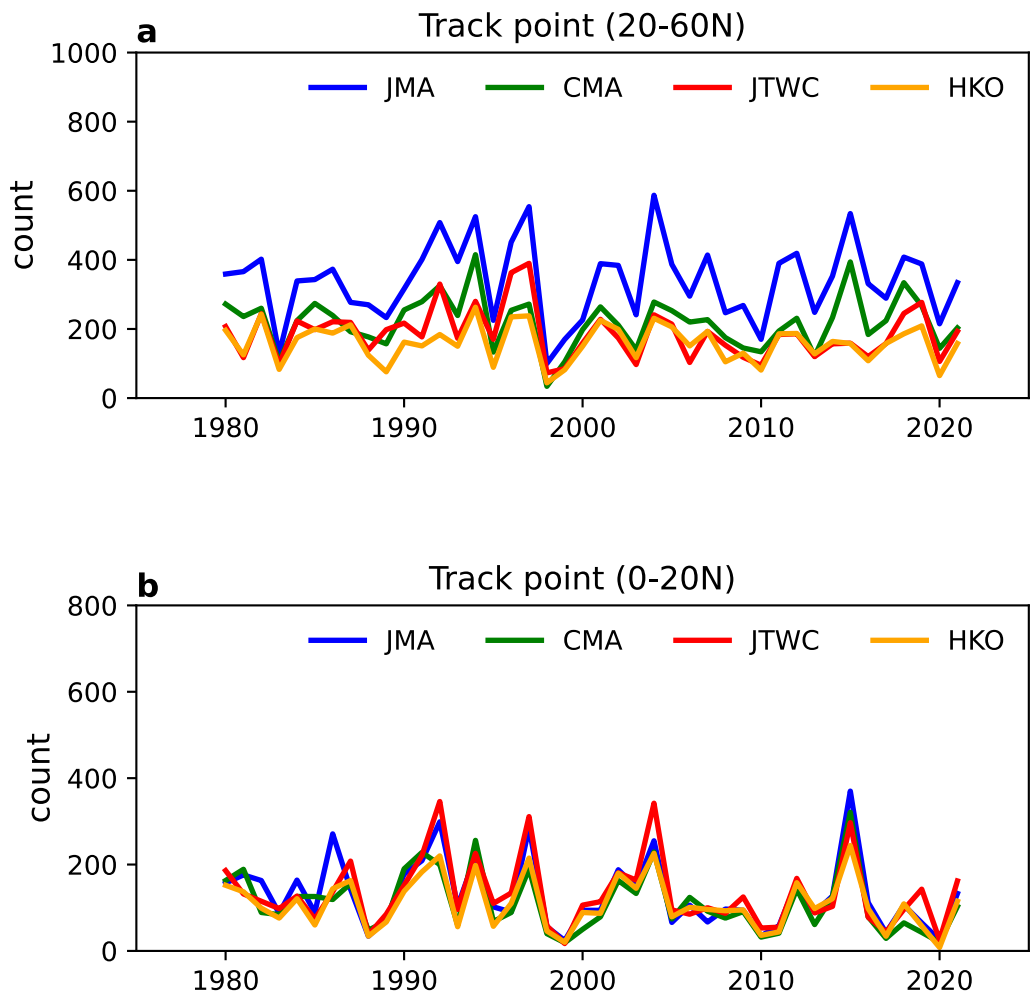

Supplementary Information Fig.S12: TC track point counts, for recurving TCs, from different Best Track data sources in the common period of 1980–2021.

a, The annual total number of track points falling within the latitudinal band of 20–60°N in the WNP, for recurving TCs only, from different Best Track data sources, including the JMA, CMA, JTWC and HKO, in the common period of 1980–2021. **b** as **a**, but for the annual total number of track points falling within the latitudinal band of 0–20°N.

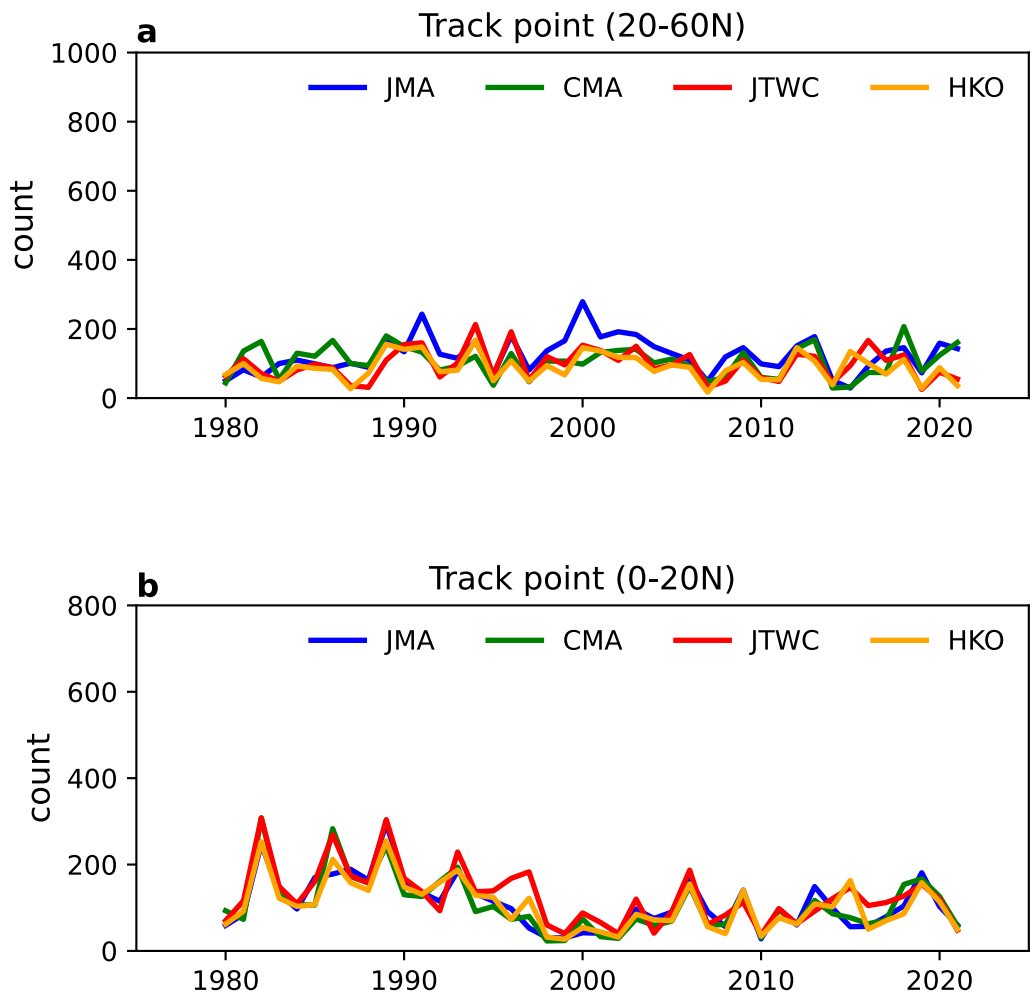

Supplementary Information Fig.S13: TC track point counts, for straight-moving TCs, from different Best Track data sources in the common period of 1980–2021.

As for SI Fig.S12, but for straight-moving TCs only.

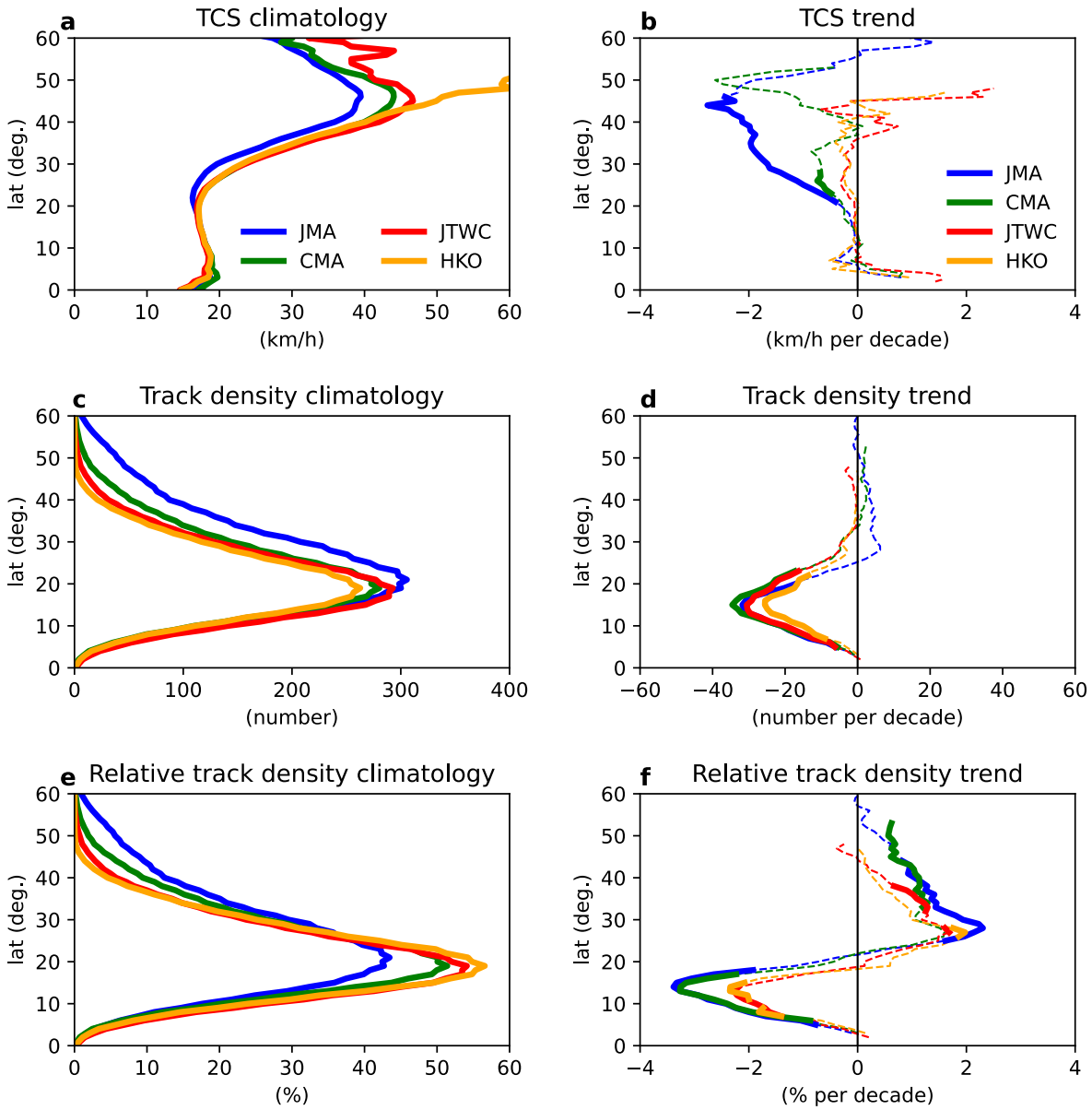

Supplementary Information Fig.S14: Climatology and long-term changes in translation speed and track density of typhoons at the latitude bands from different Best Track data sources in the common period of 1980–2021.

a, c, e, Climatology of tropical cyclone translation speed (TCS), track density, and the proportion of track density, at the 10° latitude-moving bands from 0 to 60°N in the WNP from different Best Track data sources, including the JMA, CMA, JTWC and HKO, in the common period of 1980–2021. **b, d, f,** Linear trends of TCS, track density, and the proportion of track density, at the 10° latitude-moving bands from 0 to 60°N in the WNP from different Best Track data sources, including the JMA, CMA, JTWC and HKO, in the common period of 1980–2021. In **b, d, f**, thick solid lines show significant trends at 95% confidence, thin dashed lines for insignificant trends at 95% confidence.

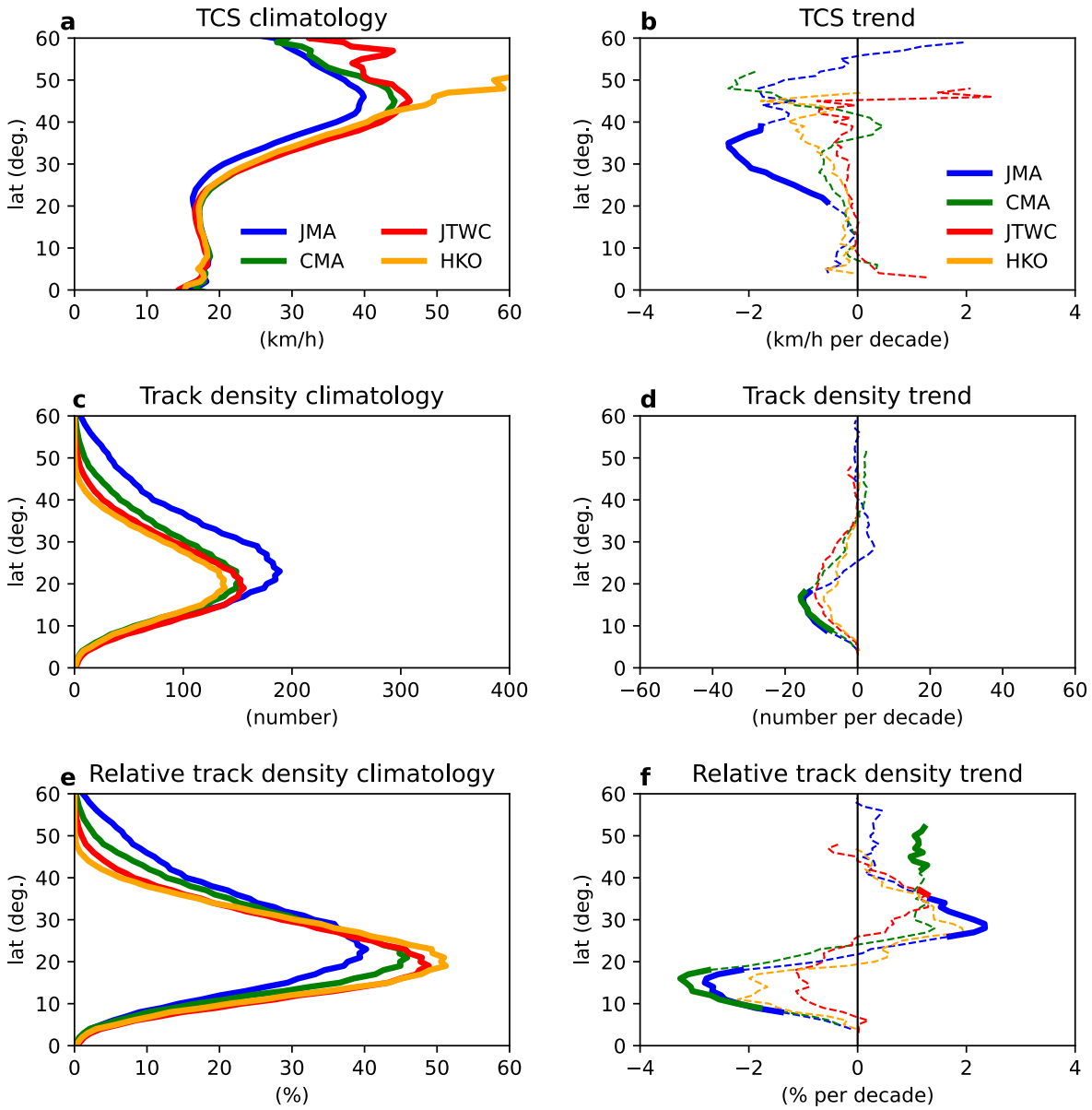

Supplementary Information Fig.S15: Climatology and long-term changes in translation speed and track density at the latitude bands, for recurving TCs, from different Best Track data sources in the common period of 1980–2021.

As for SI Fig.S14, but for recurving TCs only.

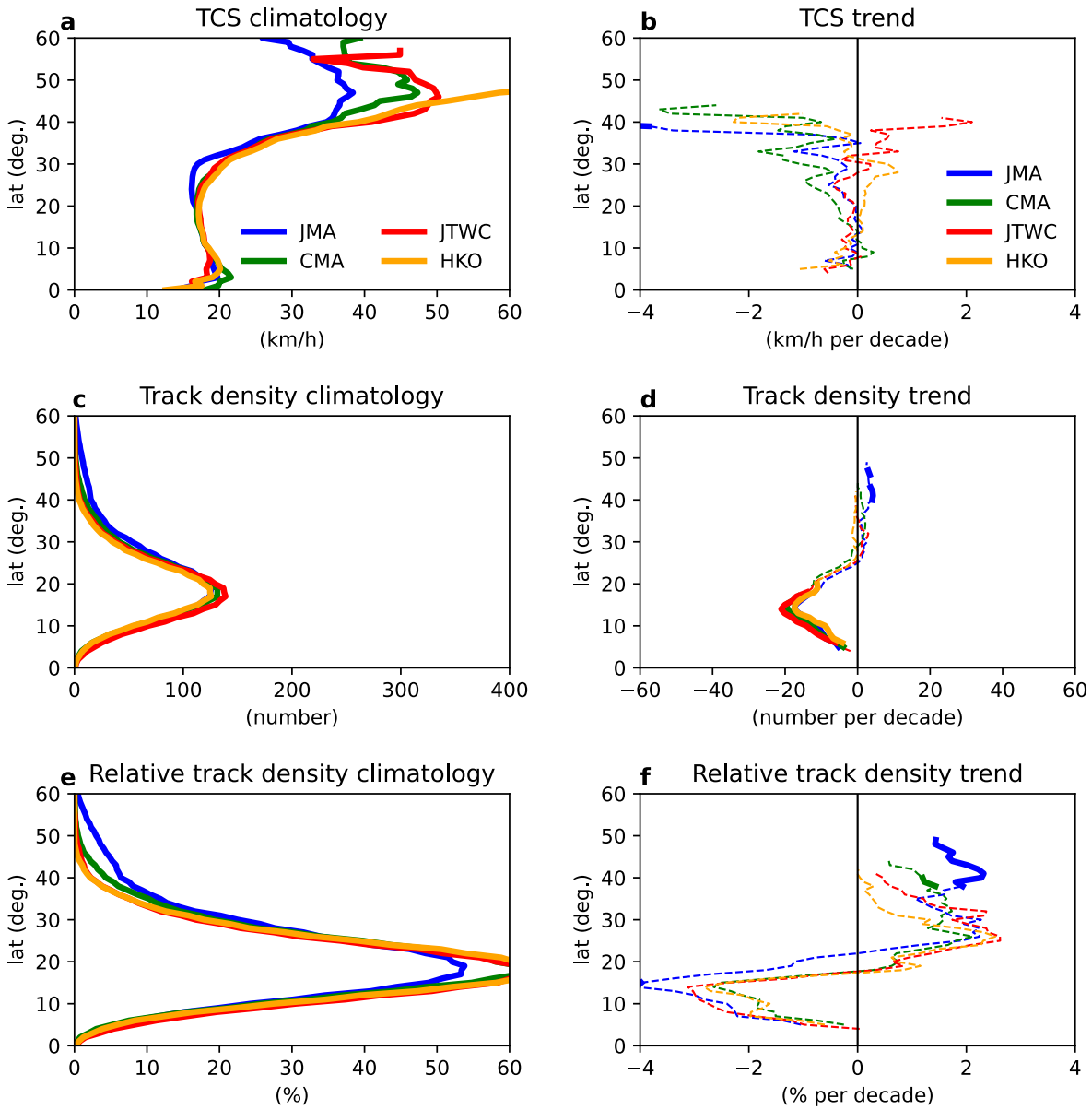

Supplementary Information Fig.S16: Climatology and long-term changes in translation speed and track density at the latitude bands, for straight-moving TCs, from different Best Track data sources in the common period of 1980–2021.

As for SI Fig.S14, but for straight-moving TCs only.